

J. Astrophys. Astr. (2001) 22, 18

GMRT detection of HI 21 cm -line absorption from the peculiar galaxy in Abell 2125

K. S. Dwarakanath¹ and F. N. Owen² ^y

¹Raman Research Institute, Bangalore 560 080, India

²National Radio Astronomy Observatory, Socorro, NM 87801, USA

Received 2000 October 27; accepted 2001 February 05

Abstract. Using the recently completed Giant Metrewave Radio Telescope, we have detected the HI 21 cm -line absorption from the peculiar galaxy C 153 in the galaxy cluster Abell 2125. The HI absorption is at a redshift of 0.2533, with a peak optical depth of 0.36. The full width at half minimum of the absorption line is 100 km s^{-1} . The estimated column density of atomic Hydrogen is $0.7 \times 10^{22} (\tau_s/100) \text{ cm}^{-2}$. The HI absorption is redshifted by 400 km s^{-1} compared to the [O III] emission line from this system. We attribute this to an in-falling cold gas, or to an out-flowing ionised gas, or to a combination of both as a consequence of tidal interactions of C 153 with either a cluster galaxy or the cluster potential.

Key words: Galaxies: active | galaxies: clusters: individual (A 2125) | galaxies: star-burst | radio lines: galaxies

1. Introduction

Abell 2125 is a rich cluster of galaxies (Abell Class 4) at a redshift of 0.246. Recently a detailed optical and radio study of this cluster was published (Dwarakanath & Owen 1999, Owen et al 1999). These studies have detected 27 radio galaxies in this cluster above a 20 cm luminosity limit of $1.4 \times 10^{22} \text{ W Hz}^{-1}$ ($H_0 = 75 \text{ km s}^{-1} \text{ Mpc}^{-1}$, $q_0 = 0.1$). In projection, these radio galaxies extend over $\sim 5 \text{ Mpc}$ along a band running from the northeast to the southwest of the cluster center. About half of these galaxies show signs of star formation, with the largest concentration of them in the southwest clump $\sim 2 \text{ Mpc}$ in projection from the cluster center. There is a bimodal distribution of the 27 cluster members in radio luminosity, with the majority

e-mail: dwaraka@rri.res.in

^ye-mail: fowen@nrao.edu

below a spectral luminosity at 20 cm of $10^{23} \text{ W Hz}^{-1}$. Star formation is primarily responsible for the radio emission of these galaxies. Rest of the members with a spectral luminosity above this value owe most of their radio emission to an AGN activity in them.

In Fig. 1 a radio image of the central region of the cluster is reproduced from Dwarakanath & Owen (1999). All the sources in this figure are cluster members. The brightest source in this figure (C153) has a peak flux density of 23.2 mJy/beam and is within $30''$ ($\sim 100 \text{ kpc}$) in projection from the cluster core. This is the second brightest radio source in the cluster with a 20 cm spectral luminosity of $3.3 \times 10^{24} \text{ W Hz}^{-1}$. Most of this radio emission arises in the core of this galaxy. The core is essentially unresolved at a resolution of $1.8''$. However, faint extended radio emission can be seen towards northwest and southeast directions. This galaxy has a ratio of $[\text{N II}]$ to $\text{H}\alpha$ consistent with an AGN (Owen et al 1999). But, the value of the continuum break around 4000 \AA ($\text{D}(4000)$), and the value of $B - R$ (color) are very small and consistent with star formation as well as AGN activity. The star formation rates implied by the $\text{H}\alpha$ and O II lines are consistent with each other but are a factor of 50 too small to account for the observed radio emission (Owen et al 1999). This discrepancy can arise either because the star formation rates are underestimated due to dust in C153, or most of the radio emission from C153 is due to an AGN activity. In comparison with the blue luminosities and colors of other cluster members where the star formation rates estimated by the optical lines and the radio continuum agree, it is apparent that dust obscuration is unlikely to be significant in C153. Most of the radio emission from C153 must therefore be due to an AGN activity at its center.

Since there is star formation and AGN activity in C153, we might expect to detect some of the cold gas feeding the AGN. Such a cold gas could be in a torus close to the nucleus. Alternatively, we might expect to detect the H I in the interstellar medium of the host galaxy. Such a system with multiple H I absorption components was indeed detected in Hydra A (Dwarakanath, Owen, & van Gorkom 1995). In-fall velocities of H I absorption components up to 400 km s^{-1} have been detected in radio elliptical galaxies (van Gorkom et al 1989, van der Hulst et al 1983, Shostak et al 1983). This in-falling H I gas has been attributed to cold gas losing its angular momentum due to frictional drag on it by the pressure supported hot gas in the ellipticals. Interactions and mergers are quite common in cluster galaxies (Lavery & Henry 1994, Dressler et al 1994, Couch et al 1994, Wirth, Koo, & Kron 1994). Such interactions can lead to disturbed morphologies and chaotic velocity fields of the interacting galaxies. In-flow and/or out-flow of ionised and/or atomic gas is expected from such galaxies. It is interesting to explore if C153 displays any such phenomena.

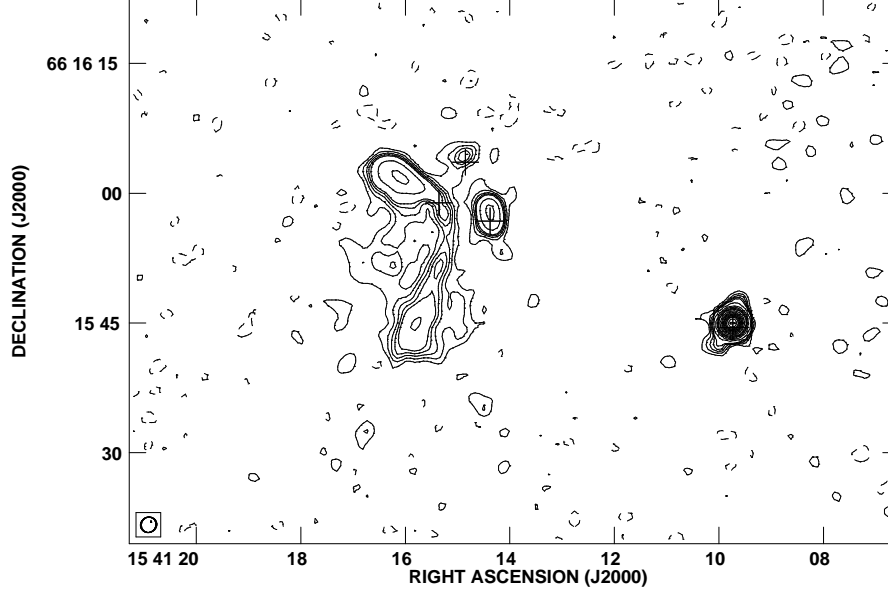


Figure 1. Radio image of the center of Abell 2125. This is a 20 cm image made with the VLA in its A configuration with a resolution $1.8''$. The crosses mark the positions of optical identifications. The brightest source in this figure (C153) has a peak continuum surface brightness of 23.2 mJy/beam and is within 100 kpc (in projection) from the cluster core. This source shows signs of star formation although it is an AGN. The rms in this image is 30 Jy/beam. The contours are in steps of 60 Jy/beam from -120 to 300 Jy/beam (excluding 0), in steps of 0.6 mJy/beam from 0.6 to 3 mJy/beam, in steps of 1.5 mJy/beam from 4.5 to 15 mJy/beam, and in steps of 3 mJy/beam from 18 to 30 mJy/beam. The synthesised beam is at the bottom left corner.

2. GMRT Observations

The Giant Meterwave Radio Telescope (GMRT) located at Khodad near Pune in India, is an aperture synthesis instrument consisting of 30 fully steerable parabolic dishes of 45 m diameter. Six antennas are distributed along each of the three arms of a rough Y and the remaining 12 antennas are more or less randomly placed in a compact cluster near the center of the Y. The center of the Y, called the ⁰Central Square⁰ has a minimum baseline of 100 m and a maximum baseline of 1 km. The maximum baseline of the GMRT array is 25 km (Swarup et al 1991). Currently the antennas have

dualpolarised feeds at 5 frequencies viz., 150, 230, 327, 610, and 1420 MHz. The 1420 MHz feed is a broad-band corrugated horn covering the frequency range of 900 – 1450 MHz continuously. The full width at half maximum of the primary beams of the GMRT dishes at 20 cm is 25° .

For the current observations the antennas were pointed at (J2000) = $15^h 41^m 09^s$ and (J2000) = $66^\circ 15' 44''$. The backend used was a 30 station FX correlator which produces 128 spectral channels across the chosen baseband bandwidth. Any bandwidth which is $2^n \times 62.5$ KHz with n taking integer values between 0 and 8 can be chosen. In the present observations, a bandwidth of 8 MHz centered at 1134 MHz was used. This 8 MHz band covered a velocity range of 2000 km s^{-1} at the redshift of 0.2526 of C153. The corresponding velocity resolution is 15.7 km s^{-1} . Although most of the 30 antennas were included in the observations, the total number of antennas that were used in the analysis was 14 with a maximum baseline of 2.5 km. The integration time on the source was 4 Hr. Gain and bandpass calibrations were carried out by observing the VLA calibrator 1634+627 once an hour. The absolute flux densities were estimated by observing 1331+305 (3C 286).

The raw data from the telescope was converted to FITS format and analysed using the Astronomical Image Processing System (AIPS) developed by the National Radio Astronomy Observatory). The channels from the part of the spectrum and which were free from line absorption were used to estimate the continuum visibilities. Spectral-line visibilities in each of the spectral channels were obtained by subtracting the estimated continuum contribution from the observed visibilities. A continuum image and a spectral cube were made using AIPS. The synthesised beam was $36'' \times 22''$ at a position angle of -22° . The r.m.s. value in the spectral cube was $1.5 \text{ mJy/beam/channel}$, close to the expected value. The spectral cube was featureless except for the absorption line in the galaxy C153. The spectral cube was Hanning smoothed with a resulting r.m.s. of $0.9 \text{ mJy/beam/channel}$. The spectrum towards C153 from this cube is displayed in Fig. 2. The velocity resolution in this spectrum is 32 km s^{-1} .

The H I absorption line is at a redshift of 0.2533, or, at a systemic velocity of 66550 km s^{-1} . The best-fit Gaussian gives a full width at half maximum of 100 km s^{-1} . The peak optical depth is 0.36 and the corresponding H I column density is $0.7 \times 10^{22} (\tau_s/100) \text{ cm}^{-2}$. The corresponding H I mass in a sphere of radius 1 kpc is $10^8 M_\odot$.

3. Discussion

The most interesting aspect of the H I absorption in C153 is that it is redshifted by 400 km s^{-1} w.r.t. the velocity of the [O III] emission line, but is within 60 km s^{-1} of the H α and [O II] emission lines (Owen, under prepa-

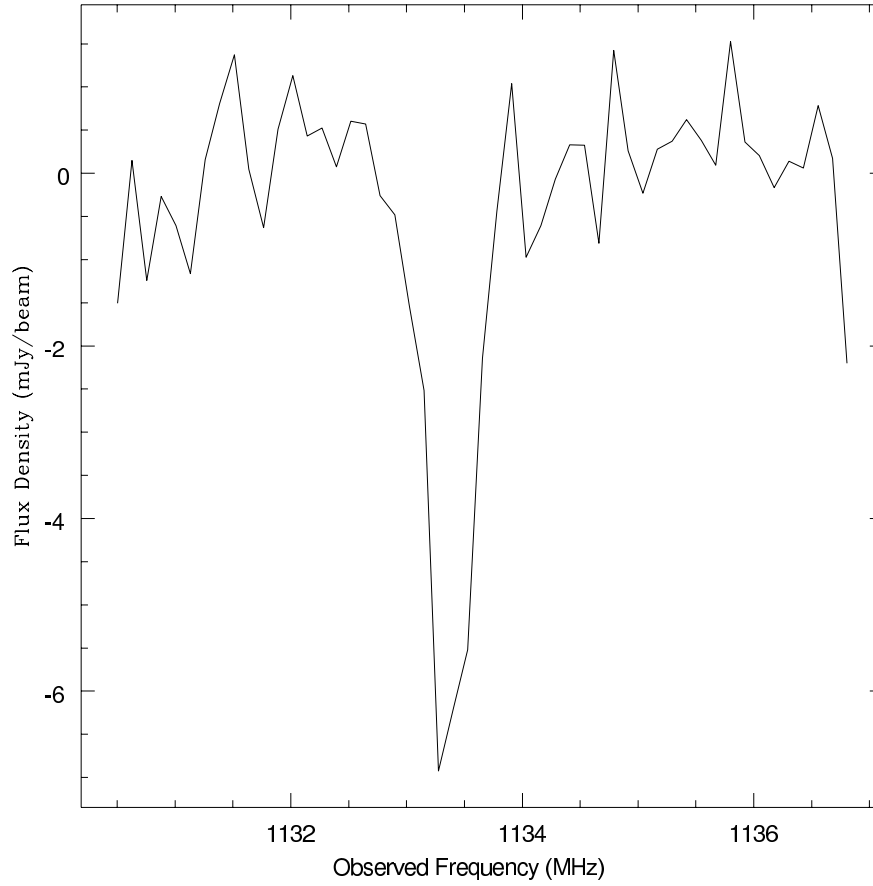


Figure 2. The HI 21 cm line absorption in A2125 obtained using the GMRT. The zero on the y-axis corresponds to the peak continuum surface brightness of A2125 of 24.1 ± 1.5 mJy/beam and is in excellent agreement with 23.2 ± 0.075 mJy/beam estimated from earlier VLA observations (Dwarakanath & Owen 1999). The spectrum was obtained at $(J2000) = 15^{\text{h}}41^{\text{m}}09.83^{\text{s}}$, and $(J2000) = 66^{\circ}15'44.1''$. The original spectrum was Hanning smoothed and alternate channels plotted to obtain the spectrum shown here with a velocity resolution of 32 km s^{-1} . The peak absorption has an optical depth of 0.36 and corresponds to a redshift of 0.2533. The [O III] emission line from this system is blue shifted w.r.t. the HI absorption line by 400 km s^{-1} .

ration). The errors in the redshift estimates based on the optical lines are expected to be 60 km s^{-1} making the velocity difference between the HI absorption line and the [O III] emission line significant. The [O II] and the [O III] line emission appear to come from a more extended, disturbed region than the HI absorption and the H emission lines. There can be different

scenarios accounting for the observed differences in the velocities and in the spatial extents of different lines. There can be an outflow of [O III] emitting gas while the H I absorption, the H α , and the [O II] lines are at rest w.r.t. the galaxy, or there can be an in-fall of the gas seen in H I absorption, H α , and [O II] lines while the [O III] emitting gas is at rest, or there can be a combination of these two situations. Any model that attempts to explain the current observations should also account for the width, and the H I column density of the absorption line. We consider the following physical models and discuss their plausibilities in the context of the current observations: (a) a gas torus close to the AGN, (b) the interstellar medium of the host galaxy, (c) an interacting, intervening cluster galaxy, and (d) tidal interactions with the cluster potential.

If the H I absorption is due to a gas torus surrounding the AGN, both the width, and the column density of the H I line can be explained. A rotating gas torus of dimensions comparable to the linear size of the central radio continuum source can easily account for the observed width of the H I absorption line. While the linear size of the radio continuum source is unknown, it is expected to be less than 1 kpc based on the earlier observations with the VLA (Dwarakanath, & Owen 1999). For e.g., a gas torus of H I density 20 cm^{-3} , and of extent 100 pc with a circular velocity 250 km s^{-1} surrounding a radio continuum source of comparable extent can account for the observed width and column density of the H I absorption line. The H I absorption will be essentially at rest w.r.t. the AGN since there is no systematic motion involved other than the circular motion of the torus. The H α emission could come from ionised part of the torus. However, the spatially extended [O II] and [O III] emission must have a different origin. Thus, a gas torus has a limited scope in explaining the current observations.

If the H I absorption is due to the interstellar medium of the host galaxy, then, for an assumed spin temperature of 100 K, the total column density of H I in the line is comparable to the integrated H I column density along the line of sight at low galactic latitudes ($|b| < 5^\circ$) in the Galaxy (Dickey & Lockman 1990). This similarity in the column densities indicates that the H I absorption in C 153 could also be due to the line of sight gas in its galaxy. However, the observed H I column density requires a near edge-on alignment of the disk of the galaxy to our line of sight which has a rather small probability. In addition, since the circular motion of the disk-gas is not expected to have any significant component of velocity along the line of sight, the H I absorption is expected at a velocity not too far from the systemic velocity. It is possible to account for some inward velocities by gravitational in-fall of the cold H I gas due to loss of angular momentum. This loss of angular momentum is due to the frictional drag on the cold gas by the surrounding hot gas (Gunn 1979). This model has been adapted by van Gorkom et al (1989) to account for the H I in-fall velocities observed in radio ellipticals. In their adaptation of this model, they assume spherical

cold clouds moving in circular orbits through pressure supported hot gas. These clouds experience a frictional drag and acquire radial in-fall velocities. Geometrical consistency demands that the radial velocity be not more than $1/(2)^{1/2}$ times the circular velocity. While small HI in-fall velocities $\sim 50 \text{ km s}^{-1}$ observed in some radio ellipticals can be explained by this model, larger HI in-fall velocities observed by them in these ellipticals must have a different origin. Note that there is one example (viz., NGC 315) of an HI absorption redshifted by $\sim 400 \text{ km s}^{-1}$ w.r.t. the systemic velocity (Shostak et al 1983). In this case, the column density is $4.6 \times 10^{20} \text{ cm}^{-2}$ and the line width is $< 5 \text{ km s}^{-1}$. These values are typical of interstellar clouds in the Galaxy. In the case of NGC 315 one is witnessing a single cloud along the line of sight which is presumably in a state of free-fall to its center. However, in the present case, the HI column density is 15 times larger, and the line is 20 times wider. This cold gas presumably has a different origin. Even if we assume that the HI absorption is at rest w.r.t. the galaxy (C 153), thus alleviating the difficulties in accounting for its large in-fall velocities, the requirement of near edge-on alignment of the galaxy to our line of sight to account for the observed HI column density makes this model less probable.

Absorption due to an intervening cluster galaxy alleviates the difficulties encountered in the two scenarios mentioned earlier. Galaxies in clusters are known to undergo interactions, and mergers. If a dwarf galaxy of HI mass $10^8 M_\odot$, and of size a few kpc is interacting, and falling into C 153, it can explain the current observations. The in-fall velocity of the dwarf will be at least as much as the escape velocity from C 153. The escape velocities from galaxies can be greater, or, of $\sim 400 \text{ km s}^{-1}$. Such an in-falling dwarf can easily explain the observed redshift of the HI absorption line, if we attribute the observed velocity difference between the HI absorption and [O III] emission to an in-falling cold HI gas. The width of the HI absorption line simply results from the rotation of the dwarf. Given a sufficient size for this dwarf of a few kpc, its alignment with the AGN need not be as critical as in the earlier scenario (case (b)) to give rise to the HI absorption. A consequence of such an interaction is a disturbed morphology of the galaxies. Indeed, C 153 shows a disturbed morphology as seen in the HST images. In addition, such an interaction can pull out gas from the outer regions of galaxies due to tidal interactions, and cause an outflow of gas. This can also account for the observed difference in the velocities of HI absorption and [O III] emission lines. However, there is one drawback in this picture. The galaxy C 153 is within $\sim 100 \text{ kpc}$ in projection from the cluster core. If C 153 is indeed close to the cluster core, i.e., no projection effects, then a dwarf galaxy in-fall into C 153 is less likely in the core of a high velocity dispersion ($\sim 900 \text{ km s}^{-1}$) cluster like Abell 2125. This drawback is less serious if C 153 were to be in the outer regions of the cluster.

If C 153 is not in the outskirts of the cluster but is indeed close to the core then we can advance the following alternative scenario. The observed

galaxy density distribution in Abell 2125 and its X-ray intensity distribution obtained from ROSAT PSPC observations are very similar (Owen et al 1999). The galaxy C 153 is within ~ 100 kpc from the peaks of these two distributions. Since C 153 has a velocity ~ 1500 km s⁻¹ w.r.t. the cluster mean and is in the dense core of the cluster, both tidal stripping and ram-pressure stripping are expected to be very effective. Recent simulations show that stripped gas quite often falls back onto the galaxy (Barnes, & Hemquist 1998, and references therein). In such a situation, redshifted H I absorption from the in-falling cold gas is expected. Alternatively, the stripping can lead to an outflow of gas which is seen in the lines of [O III] emission. Thus, this model can account for both in-falling cold gas and out-flowing ionised gas. A consequence of tidal stripping and ram-pressure stripping is a disturbed morphology of C 153 which is seen in its HST images. Future VLBA images in radio continuum and in the 21 cm-line of H I as well as imaging in the optical emission lines could throw more light on the nature of this source.

Acknowledgements

The Giant Meterwave Radio Telescope is the result of dedicated efforts of a large number of people at the National Center for Radio Astrophysics, Pune and at the GMRT site, Khodad. N.V.G. Sarmah and his team at the Ramana Research Institute, Bangalore were responsible for designing and building the broad-band 21 cm feeds and receivers for the GMRT. We thank Rajaram Nityananda and K.R. Anantharamaiah for stimulating discussions and useful comments on the paper.

References

- Barnes, J.E., & Hemquist, L., 1998, *Astrophys. J.*, 495, 187.
 Couch, W.J., Ellis, R.S., Sharples, R.M., & Smail, I., 1994, *Astrophys. J.*, 430, 121.
 Dickey, J.M., & Lockman, F.J., 1990, *Ann. Rev. Astron. Astrophys.*, 28, 215.
 Dressler, A., Oemler, A. Jr., Butcher, H.R., & Gunn, J.E., 1994, *Astrophys. J.*, 430, 107.
 Dwarakanath, K.S., Owen, F.N., & van Gorkom, J.H., 1995, *Astrophys. J. Lett.*, 442, L1.
 Dwarakanath, K.S., & Owen, F.N., 1999, *Astron. J.*, 118, 625.
 van Gorkom, J.H., Knapp, G.R., Ekers, R.D., Ekers, D.D., Laing, R.A., & Polk, K.S., 1989, *Astron. J.*, 97, 708.
 Gunn, J.E. 1979, In *Active Galactic Nuclei*, edited by C. Hazard and S. Mitton (Cambridge University, Cambridge), p213.
 van der Hulst, J.M., Golisch, W.F., & Haschick, A.D., 1983, *Astrophys. J. Lett.*, 264, L37.
 Lavery, R.J., & Henry, J.P., 1994, *Astrophys. J.*, 426, 524.

- Owen, F.N., Ledlow, M.J., Keel, W.C., & Morrison, G.E., 1999, *Astron. J.*, 118, 633.
- Shostak, G.S., van Gorkom, J.H., Ekers, R.D., Sanders, R.H., Goss, W.M., & Comwell, T.J., 1983, *Astron. Astrophys.*, 119, L3.
- Swarup, G., Ananthakrishnan, S., Kapahi, V.K., Rao, A.P., Subrahmanya, C.R., & Kulkarni, V.K., 1991, *Curr. Sci.*, 60, 95.
- Wirth, G.D., Koo, D.C., & Kron, R.G., 1994, *Astrophys. J. Lett.*, 435, L105.